Conversion gain non-linearity and its correction in hybridised near infrared detectors

Nagaraja Bezawada, Derek Ives and David Atkinson
UK Astronomy Technology Centre, Royal Observatory, Edinburgh EH9 3HJ

ABSTRACT

The conversion gain in hybridised near infrared detectors with Source Follower per Detector unit cells changes non-linearly as the signal integrates on the junction capacitance of the detector diodes[1, 2]. However, the non-linearity in the measured conversion gain as calculated from the conventional photon transfer technique (~15% in VIRGO-2K for example) is higher than the non-linearity noticed at the detector output (~4% in the same detectors). This paper presents experimental data from the VIRGO-2K, Aladdin-III and Hawaii-1RG detectors which is used to highlight this discrepancy and thus show the shortcomings of the use of the photon transfer technique with such non-linear detectors. The mechanism for the changing detector node capacitance with integrating signal is explained. A method for correcting the measured conversion gain to account for this non-linearity has been implemented on the data from the same detectors and will be presented. If not corrected, this non-linearity can be another source of error that could cause an over-estimation of the detector performance parameters (as is the case with the inter-pixel capacitance).

Keywords: Conversion gain, Photon transfer, Infrared detectors, VIRGO-2K, Hawaii-1RG and Aladdin-III

1. INTRODUCTION

It has been observed with near infrared hybridised detectors such as the Raytheon VIRGO-2K that the conversion gain in electrons per analog to digital unit (e^-/ADU) or transimpedance in $\mu V/e^-$ continuously changes as the signal integrates on the node capacitance[1, 2]. Figure 1 shows the full photon transfer curve and the apparent change in the measured conversion gain with signal level for a VIRGO-2K detector, SCA-module#31. The apparent change in the conversion gain as measured by the photon transfer technique is typically up to 15% for signal levels ranging from 20 to 70% full well capacity.

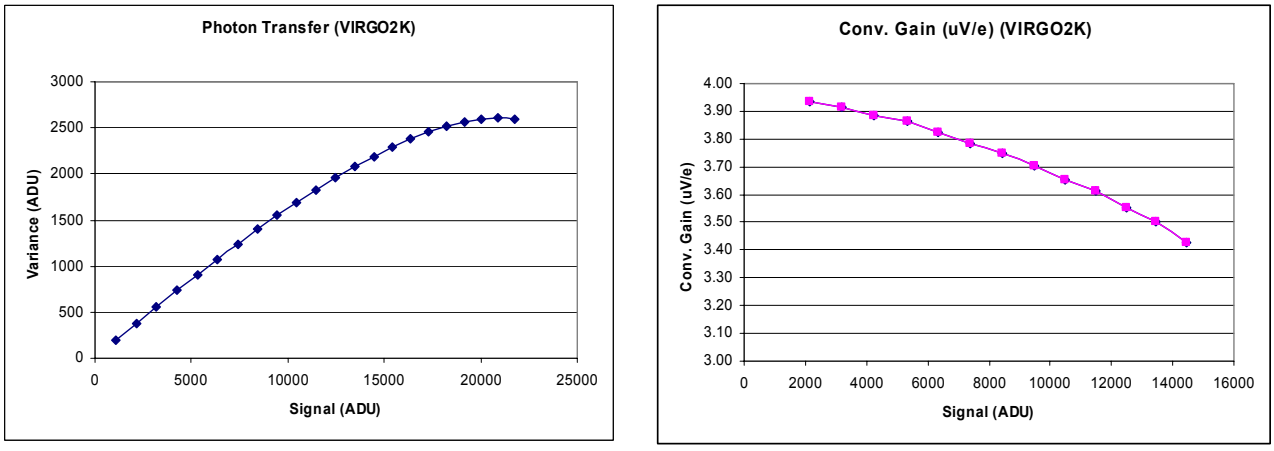

Figure 1: Left - Full photon transfer plot for VIRGO-2K. The slope of the plot is continually changing with signal. The full well (~20000 ADUs) is determined from the noise roll-over of the plot. Right - The measured transimpedance conversion gain with signal. The non-linearity in the conversion gain is ~15% from 20 – 70% of the full well.

Typically for the detectors with a Source Follower per Detector (SFD) design, the junction capacitance of the pixel diode increases as the signal integrates and this might account for the apparent change in the measured conversion gain. If it

Focal Plane Arrays for Space Telescopes III, edited by Thomas J. Grycewicz, Cheryl J. Marshall, Penny G. Warren
Proc. of SPIE Vol. 6690, 669005, (2007) · 0277-786X/07/$18 · doi: 10.1117/12.732454

were the case that the observed change in the conversion gain was entirely due to the increase in node capacitance with integrating signal, then a similar change should also be seen in the signal (ADUs) measured at the output. However, this is not the case as the non-linearity measured in the signal is only around 5% for signal levels up to 80% of full well (Figure 2) whereas the non-linearity observed in the conversion gain is around 15% from 20 – 70% of full well. This paper aims to try to explain this discrepancy by establishing the shortcomings of the conventional photon transfer measurement technique with these non-linear detectors and to provide corrections to the measured conversion gain. It also presents the effects on the detector performance parameters if the conversion gain is not corrected for the changing junction capacitance.

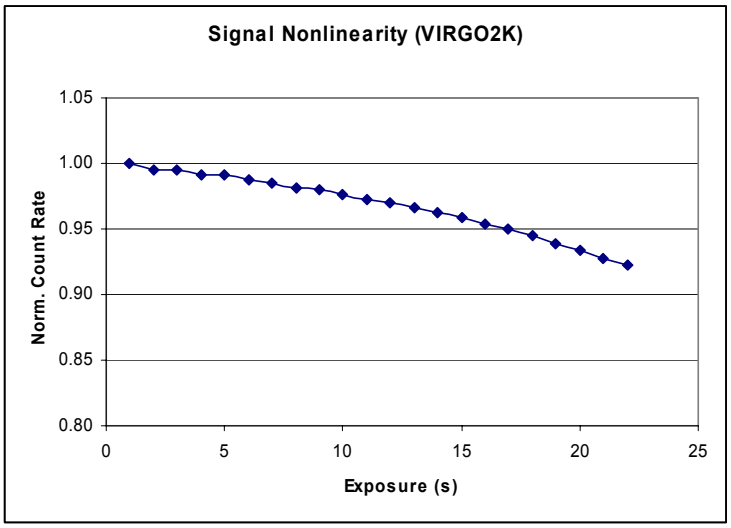

Figure 2: The non-linearity in the observed signal is only about 5% up to 80% full well. The data is obtained by varying exposure time with constant input flux.

Section 2 of this paper discusses the detector diode junction capacitance, its dependency on the applied reverse bias and a method of measuring the detector node capacitance. It also presents the non-linearity in the measured conversion gain with signal level (using the photon transfer curve) for three different detectors – VIRGO-2K, Aladdin-III and Hawaii-1RG. Section 3 discusses the limitations of the conventional photon transfer technique for non-linear devices and introduces corrections to account for the changing node capacitance with integrating signal.

2. CONVERSION GAIN

2.1 PN junction capacitance

An ideal diode is completely characterised by its I-V curve. It conducts current in the forward direction and essentially zero current in the reverse direction. There are additional characteristics in diodes due to the charge storage mechanisms. In the first instance when a junction is formed, charge is stored in the depletion region of the PN junction. The circuit manifestation of charge storage is capacitance and in the case of a PN junction is called the junction capacitance. Capacitance relates an increase in voltage to the charge stored as per the standard formula, Q=CV. The junction capacitance is essentially constant when the diode is forward biased because the potential across the diode is constant (built-in potential ~0.7V). However in the reverse bias situation the junction capacitance is not constant but depends on the applied reverse bias voltage. This is because the positive and negative charge carriers are not separated by the same fixed distance as in a real capacitor, but are pulled away from the junction creating a depletion region. As the reverse bias increases, the depletion region grows larger and the capacitance decreases because the distance between the charges increases.

The infrared detector diodes in the near infrared detectors such as VIRGO-2K, Hawaii-1RG and Aladdin-III are typically 'p-on-n' type photovoltaic detectors (see Figure 3 for VIRGO-2K detector and the unit cell architecture). The initial detector bias is set by resetting the detectors to a known reverse bias typically to 0.5 - 0.7V. The photo-generated carriers as well as dark generated carriers (holes in the case of p-on-n detectors) within the detector, charge the diode from its

initial reverse bias towards forward bias, diminishing the diode's depletion region which in turn increases the junction capacitance. So, a fully depleted diode (large reverse bias) results in a minimum junction capacitance and exhibits highest sensitivity whilst the fully discharged diode (zero bias) gives the maximum junction capacitance and exhibits lowest sensitivity.

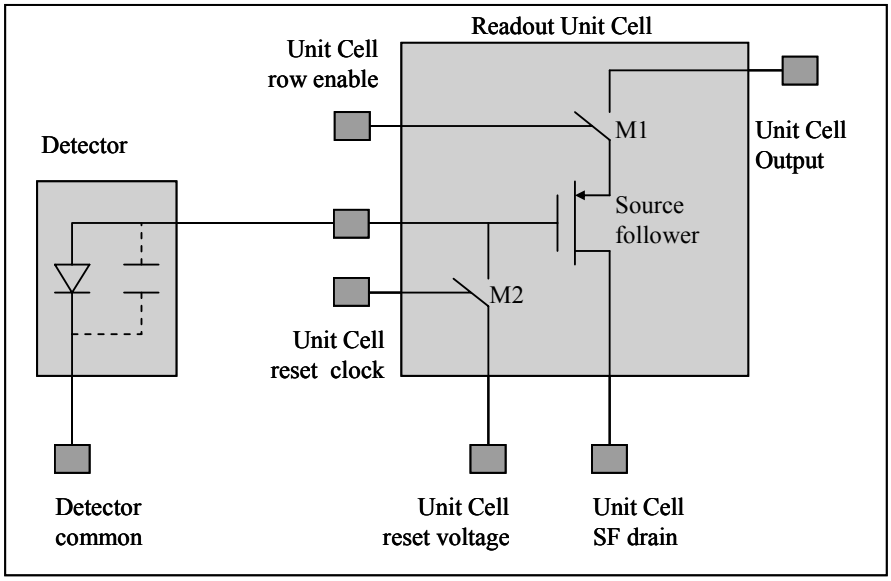

Figure 3: The detector and the unit cell (VIRGO-2K): The detectors are initially reset to a known Reset Voltage. The incoming radiation charges the diode from the initial reverse bias towards forward bias.

2.2 Node capacitance

The detector junction capacitance in parallel with the other stray capacitances associated with the gate to source of the source follower in the unit cell, together with indium bump bonds etc. determines the total detector node capacitance. The node capacitance can be determined from the following equation with the prior knowledge of the source follower gain (A_{sf}) and the conversion gain (Z_t in V/e^- units)

$$C_{node} = (1.602 \times 10^{-19} \times A_{sf})/Z_t$$

The source follower gain can be estimated by keeping the detector under reset and measuring the change in output voltage as the Reset Voltage is varied. The source follower gain is then determined by

$$A_{sf} = \Delta V_{out} / \Delta V_{RstUC}$$

The transimpedance conversion gain (Z_t) is obtained from the following equation with the knowledge of the system conversion gain (e^-/ADU) measured using the photon transfer technique[3].

$$Z_t = 1 / (\text{System Gain} \times \text{Preamp Gain} \times \text{ADC Transfer Function})$$

where, the System Gain is in e^-/ADU, the Preamp Gain is the total gain in the signal processing chain, the ADC transfer function is in ADU/V and Z_t is the transimpedance in V/e^-.

2.3 Node capacitance and the detector bias

As mentioned in section 2.1, the detector junction capacitance at the start of the integration (signal starvation) depends on the applied reverse bias. One way to measure the change in this junction capacitance with applied reverse bias is to estimate the node capacitance using the relationships mentioned in Section 2.2 at different detector biases keeping the signal levels close to the starvation level (<20% full well) but still dominated sufficiently by the photon noise. Figure 4 shows the observed system gain (left) and the corresponding node capacitance (right) with the applied detector bias for a VIRGO detector. The input flux and the integration time are kept constant and the system gain is measured at different

applied detector bias levels. The combined source follower gain (A_{sf}) has been measured as 0.94 for VIRGO detectors using the method previously described.

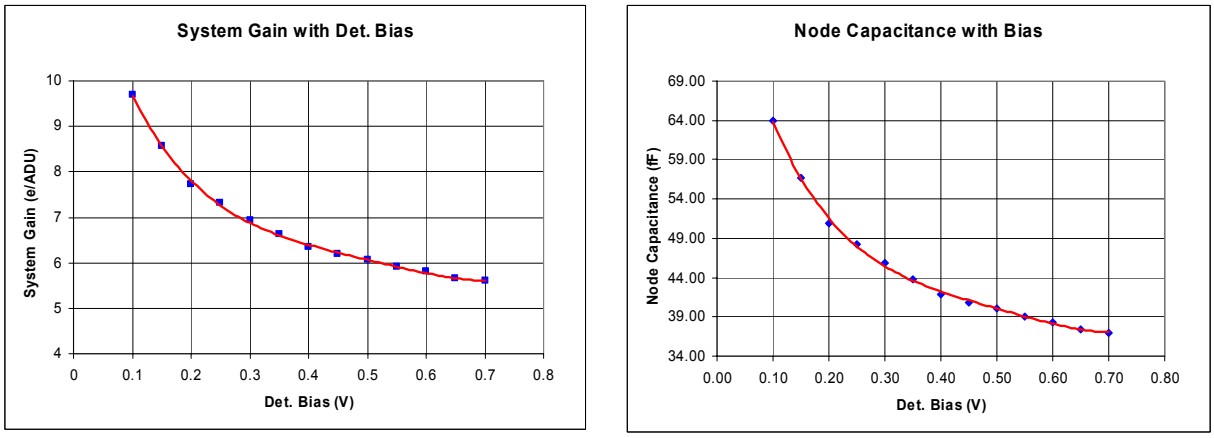

Figure 4: Left: Conversion gain (e/ADU) varies with the applied detector bias. The conversion gain is measured at low signal levels (<20% full well) using conventional photon transfer at different applied biases. Right: At each conversion gain, the corresponding node capacitance is estimated using the formulas mentioned in section 2.2. Higher reverse bias results in lower node capacitance.

2.4 Junction capacitance and integrating signal

The change in the node capacitance (due to the change in detector junction capacitance) with applied detector bias is shown above in Section 2.3. Starting at any given detector bias, the integrating signal charges the detectors towards a forward bias and so the detector bias reduces with integrating signal. Hence, a similar effect of change in the junction capacitance as shown in Figure 4 takes place. As the capacitance changes, the node sensitivity changes and so the measured system gain changes as well. This can be seen from Figure 5 (for VIRGO2K), Figure 6 (for Aladdin-III) and Figure 7 (for Hawaii-1RG) where the measured system gain (e^-/ADU) changes with the signal level (ADU). However, the change in the conversion gain (e^-/ADU) is higher than the change in the signal ADUs measured at the output. Therefore, the entire non-linearity observed in the conversion gain cannot be attributed to the changing node capacitance.

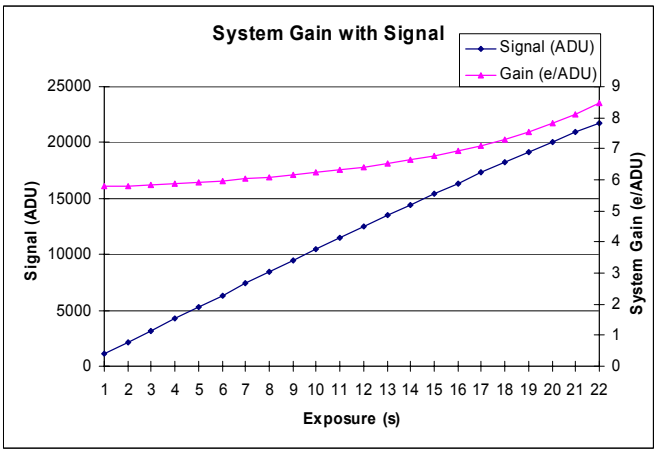

Figure 5: Signal and conversion gain for VIRGO-2K detector: Diamonds – Signal in ADU with exposure time (input flux is constant). The signal nonlinearity is ~4% up to 80% full well (Figure 2). Triangles – The conversion gain (e/ADU) measured at each signal level using conventional photon transfer. The nonlinearity in the conversion gain is ~15% from 20 – 70% of the full well signal range.

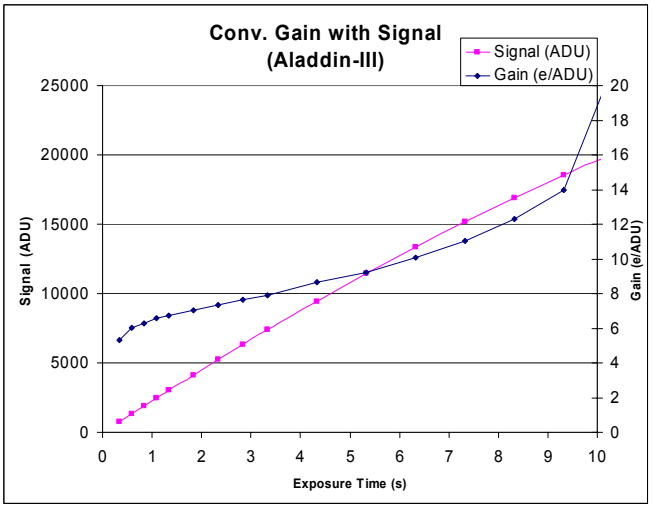

Figure 6: Signal and conversion gain for Aladdin-III detector: Squares – Signal in ADU with exposure time (input flux is constant). Diamonds – The conversion gain (e/ADU) measured at each signal level using conventional photon transfer.

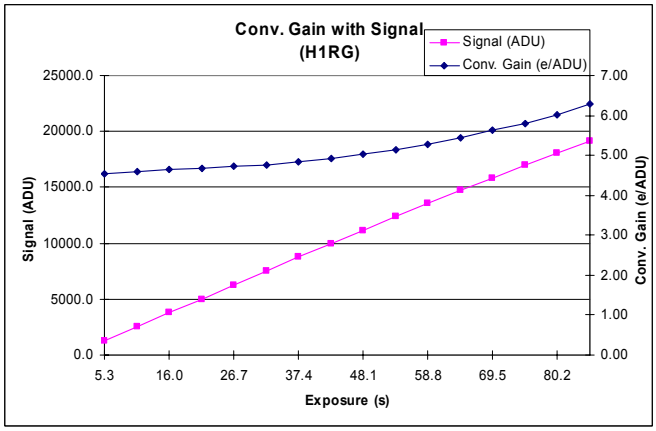

Figure 7: Signal and conversion gain for Hawaii-1RG detector. Squares – Signal in ADU with exposure time (input flux is constant). The signal nonlinearity is ~3% up to 80% full well (Figure 8). Diamonds – Conversion gain (e/ADU) measured at each signal level using conventional photon transfer. Note the nonlinearity in the conversion gain is ~13% from 20 to 70% full well.

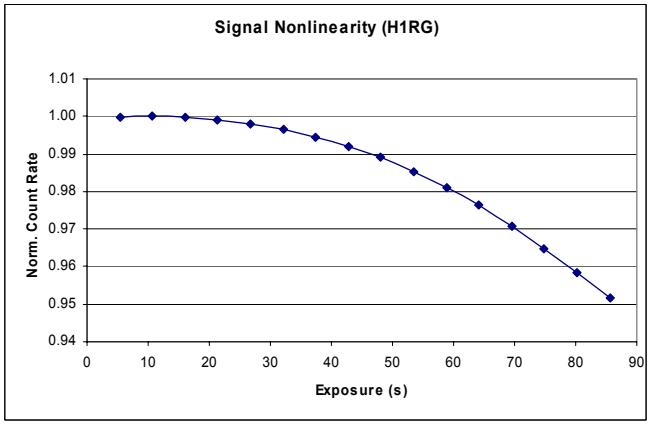

Figure 8: Signal non-linearity in the Hawaii-1RG detector. The nonlinearity is ~3% from up to 80% full well.

3. APPARENT SIGNAL

Whilst it is quick and convenient to use the photon transfer technique to estimate the conversion gain (e/ADU), the technique presents problems if the system is non-linear in the transimpedance conversion gain (V/e^-) i.e. where the sensitivity is changing with integrating signal. This is because the photon transfer technique estimates the conversion gain based on the instantaneous node capacitance at the signal level being measured and does not account for the changes in the capacitance due to integrated signal thus far. This can be verified from the data of the above plots (the example here is for the VIRGO2K) and is given below in the Table 1, by estimating the apparent signal level from the system gain (column 3) measured by the photon transfer technique. The data was obtained with constant input flux and by varying exposure times.

Table 1. The data from the plot in Figure 5.

Exposure (s)	Signal (ADU)	Gain (e/ADU)	Apparent Signal (e)	Apparent Rate (e/s)	Actual Signal (e)	Corrected Gain(e/ADU)
1	1070	5.78	6185	6184.6	6184.6	5.78
2	2135	5.8	12383	6191.5	12369.2	5.79
3	3200	5.83	18656	6218.7	18553.8	5.80
4	4256	5.87	24983	6245.7	24738.4	5.81
5	5311	5.92	31441	6288.2	30923.0	5.82
6	6354	5.97	37933	6322.2	37107.6	5.84
7	7394	6.03	44586	6369.4	43292.2	5.86
8	8432	6.09	51351	6418.9	49476.8	5.87
9	9460	6.165	58321	6480.1	55661.4	5.88
10	10473	6.23	65247	6524.7	61846.0	5.91
11	11468	6.326	72547	6595.1	68030.6	5.93
12	12484	6.418	80122	6676.9	74215.2	5.94
13	13476	6.523	87904	6761.8	80399.8	5.97
14	14455	6.644	96039	6859.9	86584.4	5.99
15	15410	6.777	104434	6962.2	92769.0	6.02
16	16378	6.933	113549	7096.8	98953.6	6.04
17	17310	7.113	123126	7242.7	105138.2	6.07
18	18255	7.303	133316	7406.5	111322.8	6.10
19	19142	7.529	144120	7585.3	117507.4	6.14
20	20040	7.807	156452	7822.6	123692.0	6.17
21	20905	8.117	169686	8080.3	129876.6	6.21
22	21750	8.464	184092	8367.8	136061.2	6.26

The instant signal (e^-) as measured by the photon transfer technique **(Signal (ADU) x Gain (e/ADU))** is shown in the column under 'Apparent Signal (e)'. The row highlighted in orange (exposure 20s) is the saturation level measured from the noise roll-over in the photon transfer curve (Figure 1). The row highlighted in blue (exposure 14s) represents ~70% of the full well capacity of the detector. The conversion gain changes by ~15% from 20 - 70% full well. As can be seen from the column 'Apparent Rate (e/s)' the rate of measured signal is increasing with signal level (or with exposure time as the input flux is kept constant). This is not expected as the input flux is kept constant for all the exposure times. The measured signal rate (e^-/s) should remain constant as the input flux is kept constant. The possibility of the blackbody source drifting is eliminated as its flux output remained constant throughout the tests. The effect of inter-pixel capacitance, which is about 3 – 5% in the VIRGO detectors[4, 5] cannot account for this ~15% of change in conversion gain as only a marginal change, about 1%, is noticed with signal as shown in Figure 9.

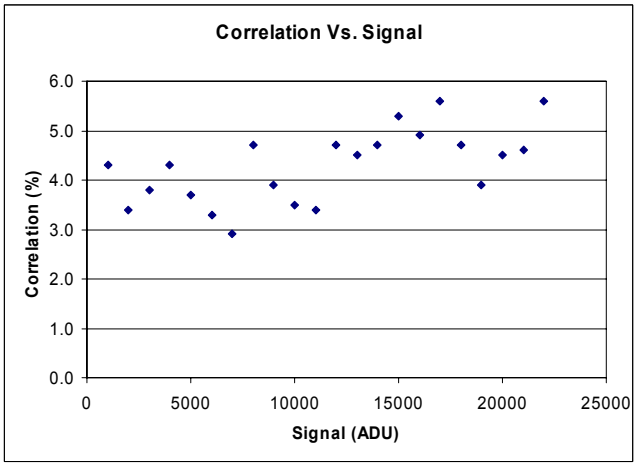

Figure 9: Correlation of pixels due to the inter-pixel capacitance shows only a marginal change (~1%) with the signal.

3.1 Actual signal and corrected gain

Janesick et al. discussed [6] the nonlinearity in 3-transistors (3-T) per pixel CMOS detectors and suggested a method to account for the nonlinearity in V/e^-. A non-linearity greater than 200% has been reported in the 3-T CMOS detectors mainly due to the same reasons described above (changing node capacitance with signal). The CMOS detectors with 5-T or 6-T per pixel CMOS detectors circumvent this problem by decoupling the charge collection and measuring node capacitances through a transfer gate built into the pixels.

The hybridised infrared detectors described here which typically use a source follower per detector structure (utilising 3 transistors per unit cell) are similar in operation to the 3-T CMOS detectors described by Janesick and so a similar method of correction to the observed gain and to estimate the actual signal is adapted here for these detectors. The correction is needed because the photon transfer technique sees the instantaneous node capacitance (junction + stray capacitance) as if it was fixed whereas the integrating signal changes this capacitance continuously. In other words, the actual input signal (the charge carriers) to charge the increasing capacitance to a certain voltage level is always less than the input signal that would be required to charge a fixed capacitance (the instantaneous capacitance – as seen by photon transfer at the signal level being measured) to the same level. So the photon transfer overestimates the signal where the capacitance is increasing on an integrating input signal. Section 3.2 illustrates this mechanism in a simple 'interest bearing bank account' analogy.

Corrections to the conventional photon transfer method to account for the V/e^- nonlinearity are calculated by first determining the signal count rate (e^-/s) for low signal levels. Then, as the signal is integrating the actual signal is determined through the knowledge that the detected signal should be directly proportional to the exposure time. The ratio of this actual signal (scaled proportionately with the exposure time) to the observed counts in ADU at the output gives the corrected gain in (e^-/ADU). Figure 10 (left) shows the plot of actual signal scaled with exposure time (based on conversion gain at low signal level) and the apparent signal that is estimated from the photon transfer technique. The error that results by using the conventional photon transfer, say at 70% full well, is approximately 11% an over-estimation of the input signal. Figure 10 right shows the detector output voltage with the signal level. As expected the output voltage measured for signals close to saturation is less than the expected voltage for the number of electrons actually present in the well. Figure 11 shows the gain corrections for Virgo-2K detector. The corrected conversion gain should be used at any given signal level in ADU to convert the ADUs into electrons. The actual signal (e) and corrected gain (e/ADU) columns of Table 1 are calculated using the method described above.

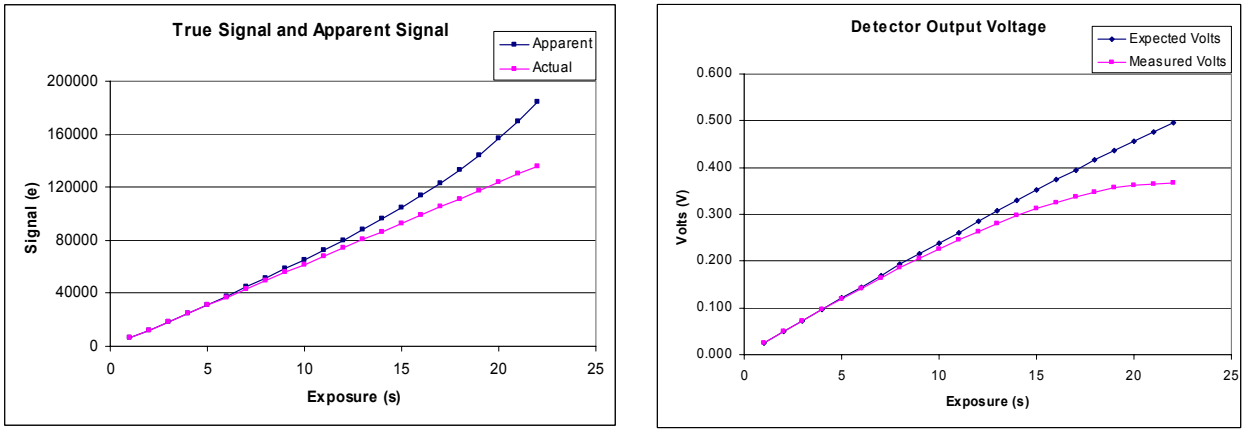

Figure 10: Left - Actual signal (scaled by the exposure time) and the apparent signal (measured by the photon transfer). Right – The expected and the measured voltage at the detector output. For the signal levels close to saturation, the measured voltage is less than the expected voltage for the number of electrons actually present in the well.

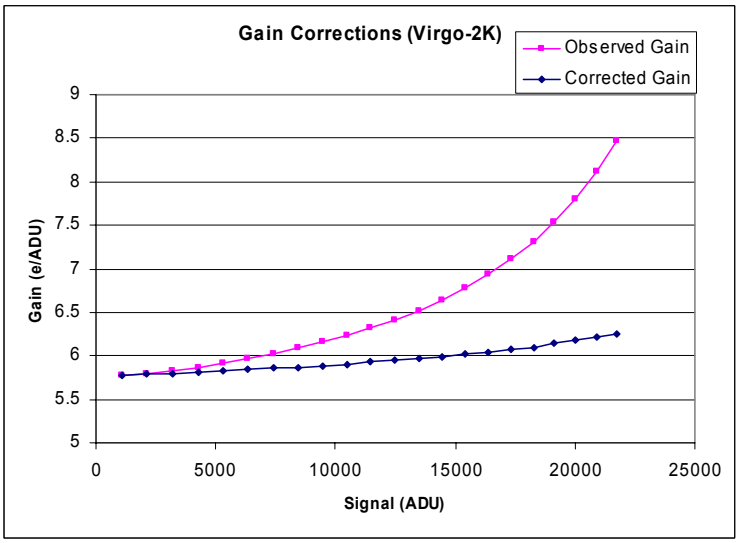

Figure 11: Gain correction in Virgo-2K detector. Diamonds: Observed gain (e/ADU) with the photon transfer. Squares: Corrected for the conversion gain errors due to the changing node capacitance. The corrected conversion gain should be used at a given signal level to avoid errors due to the nonlinear behaviour of the node capacitance.

When the corrected conversion gain is used, the non-linearity due to the capacitance change (V/e^-) and the source follower nonlinearity (V/V) are effectively removed. Corrected conversion gain should be used at the corresponding signal levels at which measurements are being obtained.

3.2 Gain corrections for Hawaii-1RG and Aladdin-III systems

Similar corrections have been performed on the observed con Similar corrections have been performed on the observed conversion gain for the Hawaii-1RG and Aladdin-III detectors. Figure 12 shows the observed gain and the corrected gain for the Hawaii-1RG detector. The error that results by using the conventional photon transfer without correcting for the changing node capacitance, say at 70% full well, is approximately 13% of over estimation of the input signal with the Hawaii-1RG detector. Figure 13 shows the observed gain and the corrected gain for the Aladdin-III detector of the UIST[7].

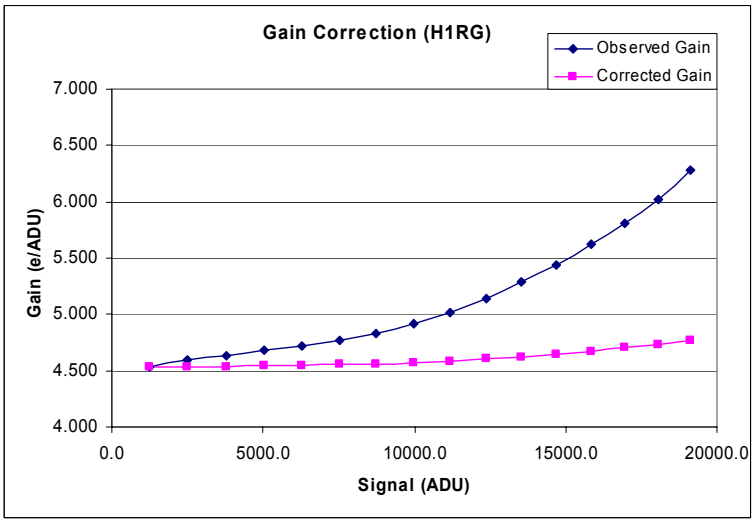

Figure 12. Gain correction in Hawaii-1RG test setup. Diamonds: Observed gain (e/ADU) with the photon transfer. Squares: Corrected for the conversion gain errors due to the changing node capacitance. The corrected conversion gain should be used at a given signal level to avoid errors due to the nonlinear behaviour of the node capacitance.

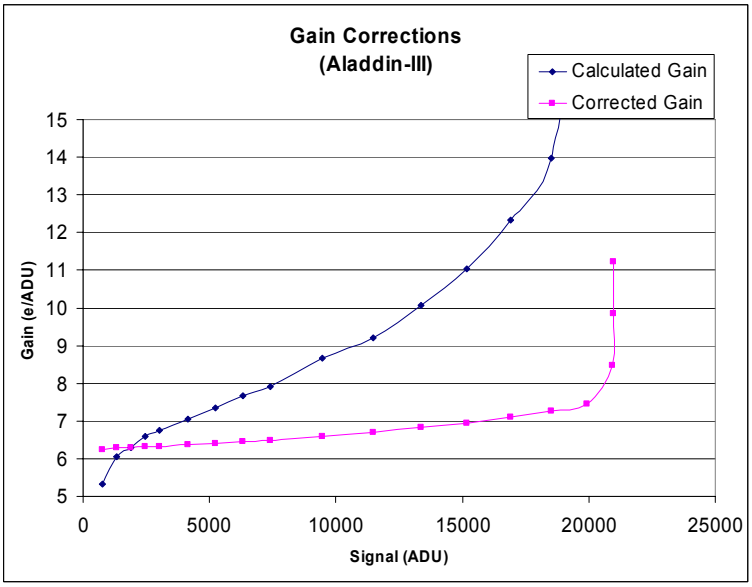

Figure 13. Gain correction in Aladdin-III test setup. Blue diamonds: Observed gain (e/ADU) with the photon transfer. Pink squares: Corrected for the conversion gain errors due to the changing node capacitance.

3.3 The bank account analogy

Apparent higher signal due to changing conversion gain can be realized through a simple bank analogy (Table 2).

A savings bank account (in pounds sterling £) = detector storing electrons;

Regular deposit (in $) = input electrons charging the detector capacitance;

Exchange rate (£ against $) = Changing capacitance leading to change in uV/e.

Assume there is a regular deposit of $10 every month (e) into the savings account (detector) which the bank converts into equivalent pounds (uV – charging the capacitance) according to the existing exchange rate (uV/e). The changing exchange rate is something similar to the changing capacitance as the signal is integrating.

Table 2. Simple bank account analogy.

Month	Deposit ($)	Ex rate ($/£)	Deposit (£)	Balance (£)	Actual ($)	Apparent ($)
1	10	1.80	5.56	5.56	10	9.99
2	10	1.82	5.49	11.05	20	20.12
3	10	1.84	5.43	16.48	30	30.34
4	10	1.86	5.38	21.86	40	40.62
5	10	1.88	5.32	27.18	50	51.08
6	10	1.90	5.26	32.44	60	61.67
7	10	1.92	5.21	37.65	70	72.26
8	10	1.94	5.15	42.80	80	83.10
9	10	1.96	5.10	47.90	90	93.91
10	10	1.98	5.05	52.95	100	104.84

$$\text{Actual}(\$) = \int_{1}^{n} (\text{Deposit}(£) * \text{Ex.rate})$$

n = 1 to no. of months. Apparent ($) = Balance (£) * Ex. rate

The actual ($) can also be computed from (No. of months x regular deposit) as the deposit amount is constant over the period. That is, the actual signal (e) can be obtained by scaling with the exposure time when the flux is constant. So, the photon transfer technique estimates the instant conversion gain (ex. rate) at the signal level being measured (balance) thus giving a higher apparent signal (apparent($)) than the actual signal (actual($)) with nonlinear devices.

3.4 Effect of non-correction

As the conversion gain is used to convert the observed ADUs to electrons, this error in the estimation of the conversion gain directly results in overestimation of the quantum efficiency, read noise, dark generation, full well capacity etc. For example, the detected quantum efficiency can easily be overestimated if we were to use just two similar signal frames at high signal levels as the detected quantum efficiency is given by

$$\text{DQE} = (S/N)^2 / S_0$$

where S is the average signal from the two similar frames, N is the noise in the frame after removing the pixel-to-pixel non-uniformity and S_0 is the estimated input signal.

$$\begin{aligned} \text{DQE} &= S\ (\text{ADU}) \times (S\ (\text{ADU}) / N^2) / S_0 \\ &= S\ (\text{ADU}) \times \text{Conversion Gain (e/ADU)} / S_0 \\ &= S\ (e^-) / S_0 \end{aligned}$$

As the measured conversion gain at high signal levels is always higher than the actual conversion gain, the QE will be overestimated. We should use the corrected gain instead of the observed gain to avoid this overestimation of the detector performance parameters. Or we should restrict the measurements to low signal levels (say <20% full well) and use the observed gain since the observed gain is close to the actual gain at low signal levels.

Similarly, the read noise, dark generation, the full well capacity etc. will also be overestimated if we use a conversion gain obtained from high signal frames. Note, we also have to correct the conversion gain for the inter-pixel capacitance which has been discussed elsewhere [4, 5], otherwise this will also lead to overestimation of the performance parameters.

4. CONCLUSIONS

The mechanism of the changing detector node capacitance with integrating signal is described and the shortcoming of the conventional photon transfer technique with nonlinear devices is explained. A method of correcting the measured

gain is adapted and implemented for the detectors such as VIRGO2K, Hawaii-1RG and Aladdin-III detectors tested at ATC. The conversion gain should be corrected for the inter-pixel capacitance as well as for the nonlinearity due to the changing node capacitance in order to avoid overestimating the performance parameters. Where possible, the conversion gain obtained using low signal frames should be used to estimate the detector performance parameters. The gain measured at high signal levels should be corrected for the changing node capacitance and then used. For the VISTA IR detectors, we have always used a conversion gain obtained at low signal levels (<20% full well) to estimate QE, read noise, dark, persistence etc in earlier reports as they are all measured at low signal levels. However, the full well capacity has been estimated using the high signal conversion gain which results in some overestimation. It is estimated that due to the conversion nonlinearity and the error with the conventional photon transfer, the full well capacity of the detectors were approximately overestimated by 7%.

ACKNOWLEDGMENTS

VISTA is funded by a grant from the UK Joint Infrastructure Fund, supported by the Office of Science and Technology and the Higher Education Funding Council for England, to Queen Mary University of London on behalf of the 18 University members of the VISTA Consortium of: Queen Mary University of London; Queen's University of Belfast; University of Birmingham; University of Cambridge; Cardiff University; University of Central Lancashire; University of Durham; University of Edinburgh; University of Hertfordshire; Keele University; Leicester University; Liverpool John Moores University; University of Nottingham; University of Oxford; University of St Andrews; University of Southampton; University of Sussex; and University College London. We would like to express our sincere thanks to Teledyne Scientific Imaging for the long term loan of an engineering grade Hawaii-1RG detector. The United Kingdom Infrared Telescope is operated by the Joint Astronomy Centre on behalf of the Science and Technology Facilities Council of the U.K.

REFERENCES

1. N. Bezawada, D. Ives, G. Woodhouse, “Characterisation of VISTA IR detectors,” SPIE Vol. 5499, 23-34 (2004)
2. N. Bezawada, D. Ives, “Performance Overview of VISTA IR Detectors,” Scientific Detectors for Astronomy 2005, ASSL Vol. 336, p.499-506
3. J. Janesick, “Scientific Charge-Coupled Devices,” SPIE Press, 2001
4. G.Finger, J. Beletic, R. Dorn, M. Meyer, L. Mehrgan, A. Moorwood, J. Stegmeir, “Conversion gain and interpixel capacitance of CMOS hybrid focal plane arrays,” Scientific Detectors for Astronomy 2005, ASSL Vol. 336
5. C. W. McMurty, T. S. Allen, A. C. Moor, W. J. Forrest, J. L. Pipher, “Characterisation of 2.5 micron HgCdTe VIRGO/VISTA detector array,” SPIE Vol. 5902 (2005)
6. J. Janesick, J. Andrews, T. Elliott, “Fundamental performance differences between CMOS and CCD imagers; Part I,” SPIE Vol. 6276, 62760M 1-19 (2006)
7. S. Ramsay Howatt, Stephen Todd, Sandy Leggett, Chris Davis, Mel Strachan, Alastair Borrowman, Maureen Ellis, Jim Elliot, David Gostick, Russel Kackley, Matthew Rippa, “The commissioning and first results from the UIST imager spectrometer, ”SPIE Vol. 5492 (2004)